Modulated photocurrents in a sandwich-cell structure: II. Influence of bias illumination intensity and carrier diffusion

2003 J. Phys.: Condens. Matter 15 5577

(http://iopscience.iop.org/0953-8984/15/32/317)

INSTITUTE OF PHYSICS PUBLISHING JOURNAL OF PHYSICS: CONDENSED MATTER

J. Phys.: Condens. Matter **15** (2003) 5577–5590 PII: S0953-8984(03)61021-0

Modulated photocurrents in a sandwich-cell structure: II. Influence of bias illumination intensity and carrier diffusion

W Tomaszewicz and P Grygiel[1]

Department of Technical Physics and Applied Mathematics, Gdansk University of Technology, Narutowicza 11/12, 80-952 Gdansk, Poland

E-mail: pgrygiel@sunrise.pg.gda.pl

Received 17 March 2003
Published 1 August 2003
Online at stacks.iop.org/JPhysCM/15/5577

Abstract

The influence of bias illumination level and carrier diffusion on the modulated photocurrents (MPCs), measured in amorphous solids in a sandwich electrode configuration, is investigated theoretically. Based on the multiple-trapping model the approximate formulae for MPCs, taking into account the mentioned physical factors, are derived. It is demonstrated that the absolute magnitude of the density of states can be determined from the MPC frequency spectra, measured at suitable bias illumination intensities. The carrier diffusion affects the MPCs solely for relatively high modulation frequencies and/or low applied voltages. The criterion for neglecting the diffusion effect is given. The corresponding frequency dependences of the photocurrent phase shift and amplitude as well as of the related quantities, calculated for the exponential trap distribution, are presented.

Notation[2]

d	sample thickness (cm)
e	elementary charge (C)
$g(x,t)$	carrier generation rate (cm^{-3} s^{-1})
k	Boltzmann constant (eV K^{-1})
$i_c(x,t)$	conduction current density (A cm^{-2})
i_{in}	injection current density (A cm^{-2})
$n(x,t)$	free carrier density (cm^{-3})
$n_t(x,t)$	trapped carrier density (cm^{-3})

[1] Author to whom any correspondence should be addressed.
[2] Also refers to I.

0953-8984/03/325577+14$30.00

$n'_t(x, t, \varepsilon)$	trapped carrier density per energy unit (cm^{-3} eV^{-1})
t	time (s)
x	distance from front electrode (cm)
C_t	carrier capture coefficient (cm^3 s^{-1})
D_0	diffusion coefficient (cm^2 s^{-1})
$E(x, t)$	electric field strength (V cm^{-1})
$I(t)$	photocurrent intensity (A)
$N_t(\varepsilon)$	trap density per energy unit (cm^{-3} eV^{-1})
N_{tot}	total density of traps (cm^{-3})
S	sample area (cm^2)
T	sample temperature (K)
T_c	characteristic temperature of exponential trap distribution (K)
V	voltage applied to sample (V)
α	dispersion parameter
α_0	coefficient of light absorption (cm^{-1})
γ	'damping coefficient' of carrier-density wave
ε	trap depth (eV)
$\varepsilon_f(x)$	quasi-Fermi level (eV)
ε_m	depth of discrete trap level (eV)
ε_0	demarcation level (eV)
κ	dielectric constant
κ_0	permittivity of free space (F cm^{-1})
μ_0	microscopic carrier mobility (cm^2 V^{-1} s^{-1})
ν_0	frequency factor (s^{-1})
φ	phase shift of carrier-density wave
ϕ_I	phase shift of MPC
σ_0	sample dc photoconductance (Ω^{-1} cm^{-1})
τ_M	Maxwell relaxation time referring to stationary sample photoconductivity (s)
$\tau_r(\varepsilon)$	mean carrier dwell time in the trap (s)
τ_0	free-carrier time of flight (s)
ω	angular frequency of light modulation (s^{-1})
ω_f	angular frequency at which ε_0 and ε_f coincide (s^{-1})
ω_n	angular frequency corresponding to MPC phase shift nth maximum (s^{-1})
ΔI_m	MPC amplitude (A)
$\Phi(x)$	carrier release-time distribution function (s^{-1})
$\tilde{\Phi}(x)$	Fourier transform of $\Phi(x)$

1. Introduction

The localized states in the forbidden energy gap of amorphous solids strongly influence their photoconductive properties. Therefore the investigation of photocurrents in amorphous materials under various experimental conditions yields useful information about the energetic density of states (DOS). One of these techniques is the modulated photocurrent (MPC) method. It consists of the carrier photogeneration or photoinjection into the sample by sinusoidally modulated light. The resulting photocurrent phase shift with respect to the modulated light and amplitude is measured, usually as a function of modulation frequency.

The MPC technique was primarily used in experiments on samples with coplanar electrodes. The theoretical description of the method, as well as the results of MPC measurements in CdS, were given by Oheda [1]. The theory has been extended by Brüggemann *et al* [2], Hattori *et al* [3, 4], Longeaud and Kleider [5, 6], Reynolds *et al* [7] as well as by Kounavis [8]. In particular, alternative approaches for the analysis of the experimental data have been developed. This method has been applied for investigating the energetic DOS profile in several amorphous solids, e.g. in a-As_2Se_3 [9] and a-Si:H [10].

The first MPC measurements in a sandwich electrode configuration have been performed by Schumm and Bauer [11] in a-Si:H in order to determine both the energetic and spatial DOS. The spatial sensitivity of this method was then investigated numerically by Brüggemann *et al* [12]. The results of the MPC measurements in a sandwich-cell structure have also been given in [13, 14] for a-Si:H, in [15] for copper phthalocyanine and in [16] for poly-(*N*-vinylcarbazole). In the papers [11, 13, 15] the modified Oheda theory has been utilized. The more rigorous theoretical descriptions have been published by Tomaszewicz [17] and Hattori *et al* [18] for the case of surface carrier photogeneration and by Grygiel and Tomaszewicz [19] for finite absorption depth of the light, generating the carriers.

In the present work we examine the influence of trap saturation, depending on the intensity of the bias illumination component, as well as the influence of the carrier diffusion on the MPCs, measured in the sandwich sample configuration. This paper constitutes a continuation of the investigations reported in [19], hereafter referred to as I. The corresponding multiple-trapping (MT) transport equations are similar to those of I and are presented here in an abbreviated manner.

2. Formulation of the problem

We shall consider here the MPC experiment, performed on the insulating sample with sandwich electrodes. Technical details can be found, for example, in [11]. The basic simplifying assumptions are:

(i) The MPCs are due to transport of one-sign excess carriers, for instance electrons. This occurs when the carriers are injected from the illuminated electrode or are generated in a thin surface layer of the sample by strongly absorbed light. These processes are, in fact, equivalent, as proved in appendix A.

(ii) Both the sample dark conductance and photoconductance are very low, to preclude screening of excess carriers by the carriers of opposite sign. In particular, the condition $\omega \gg 1/\tau_M$, with ω the angular frequency of light modulation and τ_M the Maxwell relaxation time referring to the stationary sample photoconductivity, is valid (cf I).

(iii) The electric field as well as the stationary carrier distribution in the sample are uniform. This should be the case when an external field is much higher than the space charge field. One can notice that the carrier diffusion must cause some inhomogeneities of the steady-state carrier distribution. However, for a high applied field the inhomogeneities are expected to occur only in the narrow near-electrode regions and do not affect significantly the MPC.

(iv) The process of neutralization of the opposite-sign carriers, arriving at the electrodes, is very fast.

(v) The possible energy dependences of the carrier capture coefficient and the frequency factor are ignored.

2.1. Transport equations

Subject to the above assumptions, the MT carrier transport is governed by the continuity equation:

$$\frac{\partial}{\partial x}[i_c(x,t)/e] + \frac{\partial}{\partial t}[n(x,t) + n_t(x,t)] = 0, \tag{1}$$

where

$$i_c(x,t) = e\mu_0 E_0 n(x,t) - eD_0 \frac{\partial n(x,t)}{\partial x}, \tag{2}$$

and by the equations describing the carrier trapping/detrapping kinetics:

$$\frac{\partial n'_t(x,t,\varepsilon)}{\partial t} = C_t[N_t(\varepsilon) - n'_t(x,t,\varepsilon)]n(x,t) - \frac{n'_t(x,t,\varepsilon)}{\tau_r(\varepsilon)}, \tag{3}$$

with

$$n_t(x,t) = \int_0^\infty n'_t(x,t,\varepsilon)\,\mathrm{d}\varepsilon. \tag{4}$$

Here, x denotes the distance from the front electrode of the sample, t and ε stand for the time and energy variable (ε is measured from the edge of the conduction band), $i_c(x,t)$ is the conduction current density in the sample, $n(x,t)$ and $n_t(x,t)$ are the free- and trapped-carrier densities, $n'(x,t,\varepsilon)$ and $N_t(\varepsilon)$ are the densities of trapped carriers and trapping levels per unit of energy, respectively, and $\tau_r(\varepsilon) = \nu_0^{-1}\exp(\varepsilon/kT)$ is the mean carrier dwell time in the trap (ν_0 is the frequency factor, k is the Boltzmann constant and T is the sample temperature). The remaining parameters are: e the elementary charge, μ_0 the microscopic mobility, D_0 the diffusion coefficient, C_t the capture coefficient and $E_0 = V/d$ the electric field strength (V denotes the applied voltage and d the sample thickness).

The current intensity induced in the measuring circuit is determined by the formula

$$I(t) = \frac{S}{d}\int_0^d i_c(x,t)\,\mathrm{d}x \tag{5}$$

where S is the sample area.

In order to illustrate the characteristic features of the resulting MPCs, the exponential trap distribution in the energy gap is chosen:

$$N_t(\varepsilon) = \frac{N_{tot}}{kT_c}\exp\left(-\frac{\varepsilon}{kT_c}\right) \tag{6}$$

with N_{tot} the total trap density and T_c the characteristic temperature. All the numerical results, given in the paper, have been obtained for the above DOS profile.

2.2. Linearized transport equation

In the following the carrier photoinjection is considered, since the treatment of the diffusion effect on the MPCs is then simpler. The density of the injection current, due to light intensity varying sinusoidally with time, can be expressed as

$$i_{in}(t) = i_{0in} + \Delta i_{in}\exp(\mathrm{i}\omega t) \tag{7}$$

with ω the angular modulation frequency. We shall consider here the solutions of linearized MT equations, subject to the condition $\Delta i_{in} \ll i_{0in}$. The solutions are then expected to have a form analogous to (7), e.g.

$$n(x,t) = n_0 + \Delta n(x)\exp(\mathrm{i}\omega t). \tag{8}$$

Here, $\Delta n(x)$ is the complex function that determines both the amplitude and phase of the oscillating component of carrier concentration. According to the common convention, only real parts of the solutions are of physical significance. To simplify the notation, we shall not indicate the dependence of solutions on the modulation frequency. Inserting these expressions into equations (1)–(4), retaining only the first power oscillating terms and assuming that $|\Delta n(x)| \ll |\Delta n_t(x)|$, after some calculations one obtains the differential equation

$$-D_0 \frac{d^2 \Delta n(x)}{dx^2} + \mu_0 E_0 \frac{d\Delta n(x)}{dx} + i\omega\tilde{\Phi}\Delta n(x) = 0. \tag{9}$$

Here, the function

$$\tilde{\Phi} = C_t \int_0^\infty \frac{\tau_r(\varepsilon) N_t(\varepsilon)\, d\varepsilon}{[1 + C_t n_0 \tau_r(\varepsilon)][1 + (i\omega + C_t n_0)\tau_r(\varepsilon)]} \tag{10}$$

is the Fourier transform of the carrier release-time distribution function (cf I). The boundary conditions for equation (9) depend on the problem considered and will be specified in the next sections.

Inserting formula (2) into equation (5), one obtains the following expression for the ac component of the MPC:

$$\Delta I = \frac{eS}{d}\left\{\mu_0 E_0 \int_0^d \Delta n(x)\, dx + D_0[\Delta n(0) - \Delta n(d)]\right\}. \tag{11}$$

In what follows, the solutions of equation (9) are given and the behaviour of the MPCs is examined as influenced by trap saturation and carrier diffusion.

3. The influence of bias illumination intensity on the MPCs

3.1. Expression for the MPC

In this section we shall ignore the influence of diffusion on the carrier transport, setting $D_0 = 0$. The boundary condition at an illuminated electrode has the form of $\Delta i_c(0) = \Delta i_{in}$ which, according to equation (2), results in

$$\Delta n(0) = \Delta i_{in}/e\mu_0 E_0. \tag{12}$$

Integrating equation (9) one then gets

$$\Delta n(x) = \frac{\Delta i_{in}}{e\mu_0 E_0} \exp\left(-\frac{i\omega\tilde{\Phi}x}{\mu_0 E_0}\right) \tag{13}$$

and the formula (11) for the ac component of the photocurrent is

$$\Delta I = \Delta I_0 \frac{1 - \exp(-i\omega\tau_0\tilde{\Phi})}{i\omega\tau_0\tilde{\Phi}} \tag{14}$$

with

$$\Delta I_0 = \Delta i_{in} S \tag{15}$$

and $\tau_0 = d/\mu_0 E_0$ is the free-carrier time-of-flight. The above formulae have already been obtained in [17, 18] and I. However, the influence of trap saturation on the MPCs has not been considered so far.

In the following it is convenient to introduce the functions (see [17], I)

$$\varphi = \omega\tau_0 \operatorname{Re}\tilde{\Phi}, \tag{16}$$

$$\gamma = -\omega\tau_0 \operatorname{Im}\tilde{\Phi}. \tag{17}$$

From equation (13) it results that $\Delta n(d) = \Delta n(0)\exp(-\mathrm{i}\varphi - \gamma)$. Thus, φ and γ represent, respectively, the phase and the 'damping coefficient' of the free-carrier-density wave at $x = d$. With these notations, formula (14) for the photocurrent takes the form of

$$\Delta I = \Delta I_0 \frac{1 - \exp(-\mathrm{i}\varphi - \gamma)}{\mathrm{i}\varphi + \gamma}. \tag{18}$$

3.2. Approximate formulae for the functions φ and γ

The influence of a steady-state component of the illumination intensity is characterized by the relative positions of the demarcation level ε_0 [1] and the quasi-Fermi level ε_f. These quantities are defined implicitly by $\tau_\mathrm{r}(\varepsilon_0) = 1/\omega$ and $\tau_\mathrm{r}(\varepsilon_\mathrm{f}) = 1/C_\mathrm{t}n_0$, that is

$$\varepsilon_0 = kT\ln(\nu_0/\omega), \tag{19}$$

$$\varepsilon_\mathrm{f} = kT\ln(\nu_0/C_\mathrm{t}n_0). \tag{20}$$

It is useful to define the limiting frequency

$$\omega_\mathrm{f} = C_\mathrm{t}n_0, \tag{21}$$

at which the levels ε_0 and ε_f coincide. For sufficiently high bias illumination intensity one can distinguish two ranges of modulation frequency: $\omega \gg \omega_\mathrm{f}$ and $\omega \ll \omega_\mathrm{f}$, corresponding to $\varepsilon_0 < \varepsilon_\mathrm{f}$ and $\varepsilon_0 > \varepsilon_\mathrm{f}$, respectively. In these frequency regions the expressions for φ and γ simplify considerably.

In the $\omega \gg \omega_\mathrm{f}$ domain, the factors $C_\mathrm{t}n_0\tau_\mathrm{r}(\varepsilon)$ in equation (10) for $\tilde{\Phi}$ can be omitted. For a wide distribution of localized states, varying slowly in the kT energy range, one obtains [17, 18]

$$\varphi \simeq \frac{\pi}{2}kT\tau_0 C_\mathrm{t}N_\mathrm{t}(\varepsilon_0), \tag{22}$$

and

$$\gamma \simeq \tau_0 C_\mathrm{t}\int_{\varepsilon_0}^{\varepsilon_\mathrm{f}} N_\mathrm{t}(\varepsilon)\,\mathrm{d}\varepsilon. \tag{23}$$

In this frequency region the dependence of φ and γ on the modulation frequency is determined by the DOS form and, as regards γ, by the position of the quasi-Fermi level. In particular, for the exponential trap distribution (6) and extremely low trap filling, the relationships $\varphi, \gamma \propto \omega^\alpha$ hold (with $\alpha = T/T_\mathrm{c}$ the dispersion parameter).

In the $\omega \ll \omega_\mathrm{f}$ domain, for a slowly varying distribution of localized states one gets (see appendix B)

$$\varphi \simeq kT\tau_0 C_\mathrm{t}N_\mathrm{t}(\varepsilon_\mathrm{f})\frac{\omega}{\omega_\mathrm{f}}, \tag{24}$$

$$\gamma \simeq \frac{1}{2}kT\tau_0 C_\mathrm{t}N_\mathrm{t}(\varepsilon_\mathrm{f} + kT\ln 2)\left(\frac{\omega}{\omega_\mathrm{f}}\right)^2. \tag{25}$$

Thus, in this frequency range, $\varphi \propto \omega$ and $\gamma \propto \omega^2$. Analogous formulae, referring to the MPC experiment in a coplanar sample configuration, were given by Oheda [1] as well as by Longeaud and Kleider [5]. From equations (22)–(25) it follows that the functions φ and γ change their form in the vicinity of the limiting frequency ω_f.

The above-described features are illustrated by figures 1–3. Figure 1 exhibits the plots of functions φ and γ versus ω, computed from equations (16), (17) and (10), for four positions of the quasi-Fermi level. It can be seen that in the initial frequency range the courses of the mentioned functions, particularly of γ, change with the shift of quasi-Fermi level towards the shallower traps. This reflects the progressive trap filling due to increasing bias excitation.

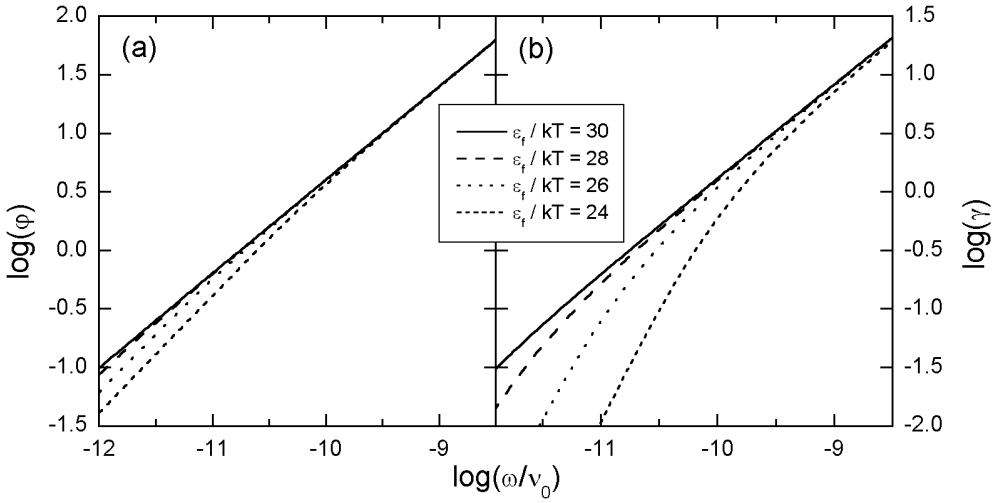

Figure 1. The phase (a) and the damping coefficient (b) of a free-carrier density wave for exponential trap distribution (6) and different positions of the quasi-Fermi level. The calculations were carried out for $\alpha = 0.8$, $\tau_0\nu_0 = 10^{-5}$ and $C_t N_{tot}/\nu_0 = 10^{13}$.

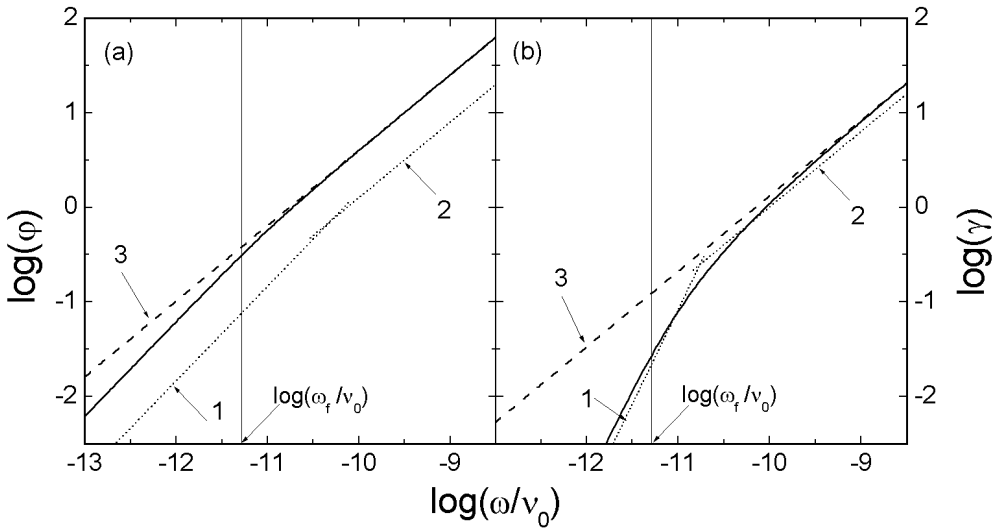

Figure 2. The phase (a) and the damping coefficient (b) of the free-carrier wave computed for the exponential distribution of traps. $\alpha = 0.8$, $\varepsilon_f/kT = 26$; other parameters are as for figure 1. Full curves represent the exact equations (16) and (17), the dotted ones marked by '1'—approximate formulae (24) or (25), the dotted curves marked by '2'—approximate formulae (22) or (23). The curves marked '3' are obtained from (16) and (17) for extremely small trap filling.

Figures 2 and 3 display the functions φ and γ versus ω, calculated for different values of the dispersion parameter α and the same quasi-Fermi level position. For the sake of comparison, the dependences computed from the exact equations (16), (17) and (10) (full curves), as well as from the approximate ones (22)–(25) (dotted curves), are presented. According to the figures, the exact and approximate functions for $\omega \ll \omega_f$ and $\omega \gg \omega_f$ differ solely in the values of multiplicative coefficients. As expected, the discrepancies diminish with decreasing parameter α, since the DOS then varies more slowly with energy.

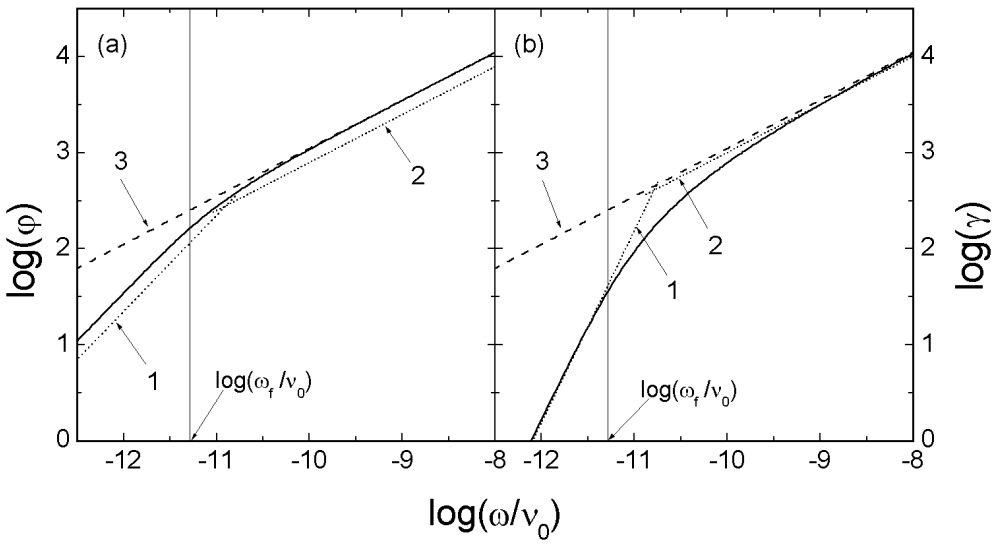

Figure 3. The phase (a) and the damping coefficient (b) of the free-carrier wave computed for the exponential trap distribution. $\alpha = 0.5$, $\varepsilon_f/kT = 26$; other parameters and notations are as for figure 2.

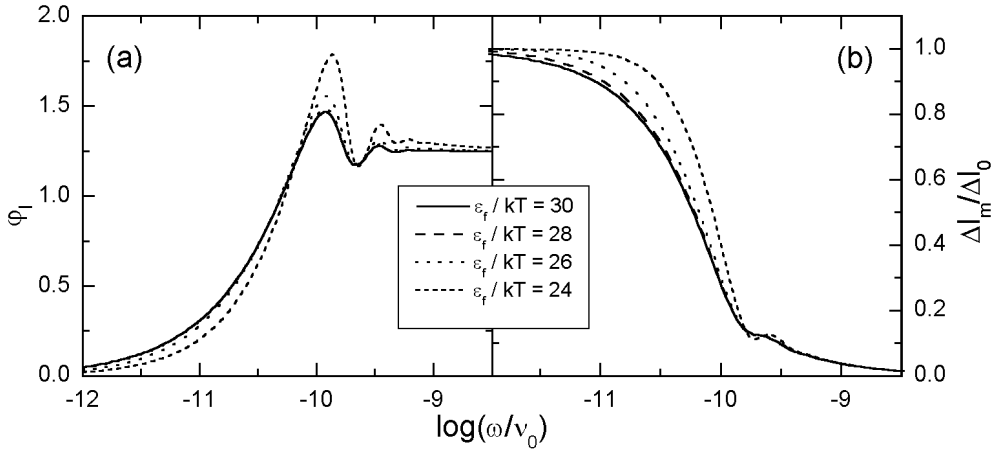

Figure 4. Frequency characteristics of the MPC phase shift (a) and amplitude (b) for exponential distribution of traps and different positions of the quasi-Fermi level. The parameters of the calculations are the same as in figure 1.

3.3. Determination of DOS from the MPCs

The measured photocurrent can be expressed as

$$\Delta I = \Delta I_{\mathrm{m}} \exp(-\mathrm{i}\phi_{\mathrm{I}}), \tag{26}$$

where ΔI_{m} and ϕ_{I} are the MPC amplitude and phase shift. Comparing this equation with equation (18), one obtains the relationships between the functions φ and γ and the functions ΔI_{m} and ϕ_{I} (cf I).

The influence of optical bias level on the MPC phase shift and amplitude is illustrated in figure 4. These quantities were calculated from equations (18) and (26) for the same positions

of the quasi-Fermi level as in figure 1. As can be seen, with increasing trap saturation the damped oscillations of ϕ_I become more and more distinct and their maxima slightly shift towards higher frequencies. This indicates that the carrier transport becomes less and less dispersive (cf I). Figure 4(b) shows that, for sufficiently high optical bias level, $\Delta I_m \simeq \Delta I_0$ in the low-frequency range which allows us to determine the value of ΔI_0 from experimental data.

In order to obtain information about the DOS one has to determine first the dependence of the functions φ and γ on the modulation frequency from the measured frequency characteristics of the MPC phase shift ϕ_I and amplitude ΔI_m. This can be done with the use of numerical methods from the overall courses of the MPCs or with the aid of the approximate formulae, valid in certain frequency domains (see [17, 18] and I). Next, the energetic DOS may be determined from the approximate equations (22)–(25). It should be noticed that

$$\frac{C_t}{\mu_0} = \frac{e\omega_f}{\sigma_0}, \tag{27}$$

where $\sigma_0 = e\mu_0 n_0$ is the sample dc photoconductance. Since the value of ω_f can be estimated from the frequency characteristics of φ and γ, obtained for sufficiently high steady-state illumination intensity, the approximate value of C_t/μ_0 can also be found. It is thus seen that equations (22) and (23), valid for $\omega \gg \omega_f$, enable us to calculate $N_t(\varepsilon_0)$ and $\int_{\varepsilon_0}^{\varepsilon_f} N_t(\varepsilon)\,d\varepsilon$, respectively. On the other hand, equations (24) and (25), being valid for $\omega \ll \omega_f$, make it possible to calculate, respectively, $N_t(\varepsilon_f)$ and $N_t(\varepsilon_f + kT\ln 2)$. Therefore the energetic DOS can be found both from the frequency characteristics of φ and γ in the region $\omega \gg \omega_f$ as well as from the dependence of these characteristics on bias intensity for $\omega \ll \omega_f$. Analogous treatment has been proposed for the MPCs measured in a coplanar sample configuration [5, 8].

In order to determine the energy scale, i.e. the actual positions of ε_0 and ε_f levels in the energy gap, the value of the frequency factor ν_0 must be known. This value can be estimated on the basis of temperature dependences of the ϕ_I and/or ΔI_m frequency characteristics and several ways could be proposed. We shall consider here the frequency region $\omega \gg \omega_f$ and assume that the temperature dependences of $C_t T/\mu_0$ and C_t/μ_0 in equations (22) and (23) are negligible. In this case the quantities φ and γ and, as a consequence, ΔI_m and ϕ_I depend on the temperature only via the demarcation energy ε_0 and the approximate scaling laws hold:

$$\phi_I = \phi_I[T\ln(\omega/\nu_0)], \tag{28}$$

$$\Delta I_m = \Delta I_m[T\ln(\omega/\nu_0)]. \tag{29}$$

Therefore, the plots of ϕ_I and ΔI_m versus $T\ln(\omega/\nu_0)$, obtained from the MPC measurements at different temperatures, should almost superimpose, which allow us to determine the value of ν_0. The mentioned scaling property is illustrated by figure 5. In calculations of ϕ_I and ΔI_m the negligible trap occupancy, $\varepsilon_f \to \infty$, was assumed and the possible temperature dependence of C_t/μ_0 was ignored. One can conclude that the scaling law for ΔI_m is better fulfilled than that for ϕ_I. The deviations follow from the approximate character of equations (22) and (23) and from the presence of the multiplicative factor T in the former equation.

4. The influence of carrier diffusion on MPCs

4.1. Expression for the MPC

The general solution of the transport equation (9), taking into account the carrier diffusion, has the form of

$$\Delta n(x) = C_1\exp(-\lambda_1 x) + C_2\exp(-\lambda_2 x). \tag{30}$$

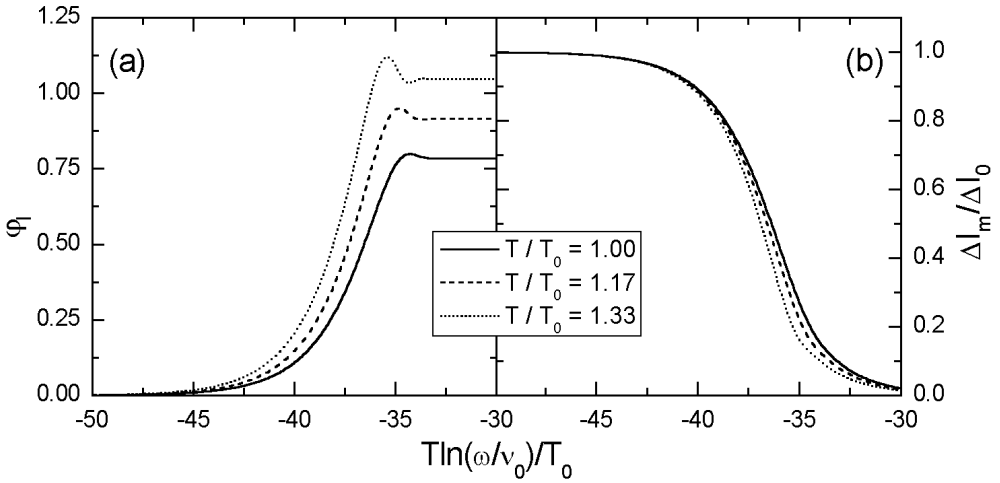

Figure 5. The frequency dependences of the MPC phase shift (a) and amplitude (b) for the exponential trap distribution and different temperatures, plotted versus $T\ln(\omega/\nu_0)/T_0$. The parameter $T_0/T_c = 0.5$: other parameters are the same as in figure 1.

The coefficients λ_1 and λ_2 are the roots of the characteristic equation

$$D_0\lambda^2 + \mu_0 E_0\lambda - \mathrm{i}\omega\tilde{\Phi} = 0 \tag{31}$$

and are given by

$$\lambda_{1,2} = \left(\pm\sqrt{\mu_0^2 E_0^2 + 4\mathrm{i}D_0\omega\tilde{\Phi}} - \mu_0 E_0\right) \Big/ 2D_0. \tag{32}$$

By the $\sqrt{z}$ function we mean here its branch, fulfilling the condition $\lim_{z\to r}\sqrt{z} = +\sqrt{r}$ (z and $r > 0$ stand for the complex and real variable, respectively).

The coefficients C_1 and C_2 in the solution (30) have to be determined from the suitable boundary conditions. According to equation (2) the boundary condition at the illuminated electrode, $\Delta i_c(0) = \Delta i_{in}$, now takes the form of

$$\mu_0 E_0 \Delta n(0) - D_0 \frac{\mathrm{d}\Delta n(x)}{\mathrm{d}x}\bigg|_{x=0} = \frac{\Delta i_{in}}{e}. \tag{33}$$

From the physical point of view, the second boundary condition should be formulated at the collecting electrode, for $x = d$. The corresponding solution, concerning the case of very fast carrier neutralization, is given in appendix C. However, a much simpler solution is obtained subject to the condition that the oscillating term of the free-carrier density vanishes at infinite distance from the illuminated electrode:

$$\lim_{x\to\infty} \Delta n(x) = 0. \tag{34}$$

Since, as can be shown, $\mathrm{Re}\,\lambda_1 > 0$ and $\mathrm{Re}\,\lambda_2 < 0$, the above condition implies that $C_2 = 0$ in the solution (30). Then, from the condition (33) one obtains $C_1 = -\Delta i_{in}/eD_0\lambda_2$ and the expression (30) takes the form of

$$\Delta n(x) = -\frac{\Delta i_{in}}{eD_0\lambda_2}\exp(-\lambda_1 x). \tag{35}$$

According to equation (11), the resulting formula for the ac term of the photocurrent is

$$\Delta I = -\frac{\Delta I_0}{\lambda_2 d}\left(\frac{\mu_0 E_0}{D_0\lambda_1} + 1\right)[1 - \exp(-\lambda_1 d)], \tag{36}$$

with the current intensity ΔI_0 given by equation (15).

4.2. Criterion for omitting the carrier diffusion

Formula (36) for MPC seems too complicated to be useful for determination of the DOS. However, it enables us to establish the criterion for omitting the influence of carrier diffusion. Let us assume the electric field strength E_0 being so high that the inequalities

$$\operatorname{Re}\tilde{\Phi},\ \operatorname{Im}\tilde{\Phi} \ll \mu_0^2 E_0^2/\omega D_0 \tag{37}$$

are fulfilled in the frequency region considered. Then the coefficients λ_1 and λ_2, given by the formula (32), are approximately equal to

$$\lambda_1 \simeq \frac{\mathrm{i}\omega\tilde{\Phi}}{\mu_0 E_0}, \tag{38}$$

$$\lambda_2 \simeq -\frac{\mu_0 E_0}{D_0}. \tag{39}$$

It can be seen that formulae (35) and (36) for the oscillating components of free carrier density and photocurrent reduce then to formulae (13) and (14), in which the carrier diffusion is ignored. Thus, the inequalities (37) are the sufficient conditions for neglecting the diffusion effects. Taking into account the definitions (16) and (17) of φ and γ as well as the Einstein relationship,

$$\frac{\mu_0}{D_0} = \frac{e}{kT}, \tag{40}$$

from (37) one gets the conditions

$$\varphi, \gamma \ll eV/kT. \tag{41}$$

This criterion, derived in a less rigorous way, was primarily given in [17]. In experimental practice usually $eV/kT \gg 1$. As shown in I, for the frequency ω_1, corresponding to the first maximum of the MPC phase shift ϕ_I, the functions $\varphi \simeq 1$ and $\gamma \simeq 1$. Therefore, from the conditions (41) it results that the carrier diffusion affects mainly the MPC courses for relatively high modulation frequencies, $\omega \gg \omega_1$.

In figure 6 the MPC courses, obtained from equation (36) for different values of the parameter eV/kT, and the case of negligible trap filling are shown. It is understood that separate curves refer to samples of different thicknesses, so that the carrier time-of-flight τ_0 remains constant. One can see that the diffusion effects are significant only for relatively low voltages, $eV/kT \lesssim 4 \times 10^2$, and are more pronounced in the high-frequency region. With decreasing voltage the oscillations of ϕ_I are more and more strongly damped, whereas the courses of ΔI_m remain almost unaffected. For extremely low values of $eV/kT = 4$ one observes only a single wide maximum of ϕ_I and a marked increase of the ΔI_m values in the high-frequency region.

Figure 7 displays the spatial distributions of free carriers, obtained for the frequency ω_1, corresponding to the first maximum of ϕ_I in figure 6(a). The curves have been computed from the formulae (35) as well as (C.2) for several values of the reduced voltage eV/kT. As can be seen, the diffusion significantly influences the carrier distribution only for relatively low voltages. The differences in the carrier concentration at the illuminated electrode are due to the phase shift of $\Delta n(0)$ with respect to Δi_in. With decreasing voltage the length of the carrier density wave increases and the wave damping becomes more and more strong. The discrepancies in the spatial distributions of the carriers calculated from equations (35) and (C.2), which refer to different boundary conditions, decrease with rising values of eV/kT and are meaningful only for $eV/kT \lesssim 40$. This indicates that the form of the boundary conditions does not have a significant influence on the MPCs, except for extremely low voltages.

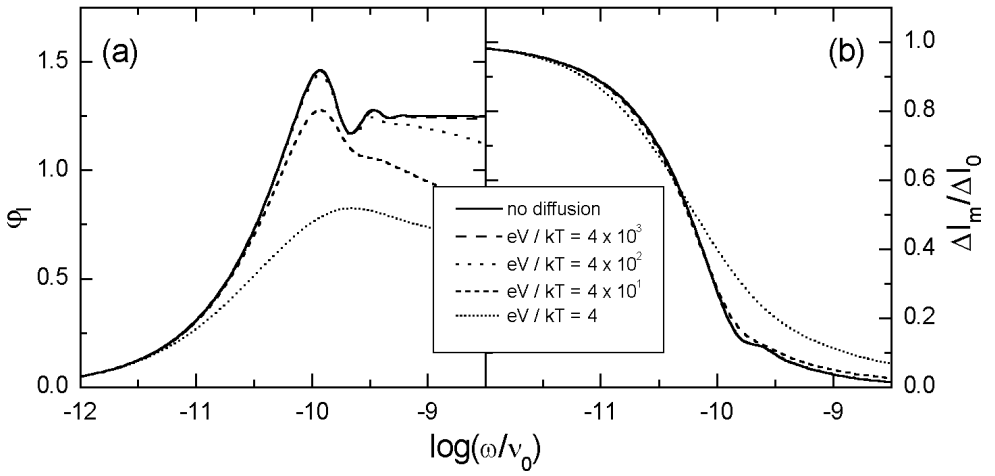

Figure 6. The MPC phase shift (a) and amplitude (b) for the exponential trap distribution and different values of the relative voltages. The remaining parameters are as for figure 1.

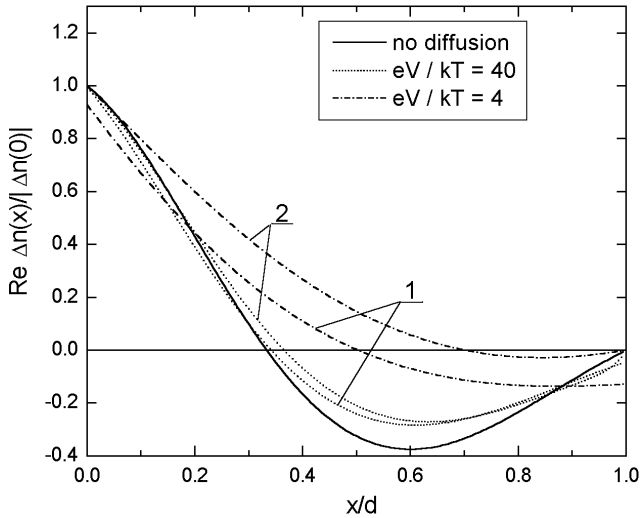

Figure 7. The spatial distribution of free carriers (real parts of oscillating terms) computed for different relative voltages. The curves marked by '1' were calculated from (35), while those marked by '2' were from (C.2). The parameters are as for figure 1.

5. Conclusions

In this paper we have investigated the influence of bias illumination intensity and carrier diffusion on the MPCs. The results given concern the photocurrents following the carrier photoinjection or surface generation. It has been shown that the measurements of the MPC frequency characteristics in suitable ranges of optical bias level and temperature enable us to determine the absolute values of the DOS and the values of C_t/μ_0 and ν_0. The DOS profile can be determined from the frequency courses of the functions φ and γ, obtained for $\omega \gg \omega_f$, as well as from their steady-state illumination dependences for $\omega \ll \omega_f$. It should be recalled that the form of DOS can also be found from the dependence of the position of the MPC phase shift maxima on the applied voltage and/or sample thickness (cf I). The carrier diffusion

significantly affects the MPCs only for relatively low values of applied voltage and/or for relatively high modulation frequencies.

Appendix A. Equivalence of carrier photoinjection and carrier photogeneration in a thin surface layer of the sample

In the case of electron photoinjection, yielding the injection current density $i_{\mathrm{in}}(t)$, integration of the continuity equation (1) with the boundary condition $i_{\mathrm{c}}(0,t) = i_{\mathrm{in}}(t)$ gives

$$i_{\mathrm{c}}(x,t)/e + \frac{\mathrm{d}}{\mathrm{d}t}\int_0^x [n(x',t) + n_{\mathrm{t}}(x',t)]\,\mathrm{d}x' = i_{\mathrm{in}}(t)/e. \tag{A.1}$$

On the other hand, for the case of carrier photogeneration the continuity equation for the electron densities has the form of

$$\frac{\partial}{\partial x}[i_{\mathrm{c}}(x,t)/e] + \frac{\partial}{\partial t}[n(x,t) + n_{\mathrm{t}}(x,t)] = g(x,t), \tag{A.2}$$

with $g(x,t)$ the carrier generation rate. If the carriers are generated in a thin near-electrode layer, the electron–hole recombination as well as the contribution of the hole current component to the MPC can be neglected. For surface carrier generation the function $g(x,t)$ can be expressed as

$$g(x,t) \simeq d\bar{g}(t)\delta(x - 0+), \tag{A.3}$$

where $\bar{g}(t)$ denotes the spatial average of $g(x,t)$ and $\delta(\cdots)$ is the Dirac delta function. Then, integration of equation (A.2) with the boundary condition $i_{\mathrm{c}}(0,t) = 0$ yields

$$i_{\mathrm{c}}(x,t)/e + \frac{\mathrm{d}}{\mathrm{d}t}\int_0^x [n(x',t) + n_{\mathrm{t}}(x',t)]\,\mathrm{d}x' = d\bar{g}(t), \qquad x > 0. \tag{A.4}$$

From the comparison of equations (A.1) and (A.4) it follows that both considered processes are equivalent, provided that

$$i_{\mathrm{in}}(t) = ed\bar{g}(t). \tag{A.5}$$

Appendix B. Approximation of functions Re $\tilde{\Phi}$ and Im $\tilde{\Phi}$ in the $\omega \ll \omega_{\mathrm{f}}$ domain

Calculating the real and imaginary parts of the function $\tilde{\Phi}$ given by equation (10), and taking into account the inequality $\omega \ll \omega_{\mathrm{f}} = C_{\mathrm{t}} n_0$, one obtains:

$$\mathrm{Re}\,\tilde{\Phi} \simeq C_{\mathrm{t}} \int_0^\infty \frac{\tau_{\mathrm{r}}(\varepsilon) N_{\mathrm{t}}(\varepsilon)\,\mathrm{d}\varepsilon}{[1 + \omega_{\mathrm{f}}\tau_{\mathrm{r}}(\varepsilon)]^2}, \tag{B.1}$$

$$\mathrm{Im}\,\tilde{\Phi} \simeq -\omega C_{\mathrm{t}} \int_0^\infty \frac{\tau_{\mathrm{r}}^2(\varepsilon) N_{\mathrm{t}}(\varepsilon)\,\mathrm{d}\varepsilon}{[1 + \omega_{\mathrm{f}}\tau_{\mathrm{r}}(\varepsilon)]^3}. \tag{B.2}$$

The factors $\tau_{\mathrm{r}}(\varepsilon)/[1 + \tau_{\mathrm{r}}(\varepsilon)]^2$ and $\tau_{\mathrm{r}}^2(\varepsilon)/[1 + \tau_{\mathrm{r}}(\varepsilon)]^3$ in the integrands are the peaked functions of ε, achieving their maxima for $\varepsilon = \varepsilon_{\mathrm{f}}$ and $\varepsilon_{\mathrm{f}} + kT\ln 2$, respectively. If the trap density $N_{\mathrm{t}}(\varepsilon)$ varies slowly with energy compared to these functions and $\omega_{\mathrm{f}} \ll \nu_0$, the integrals in (B.1) and (B.2) can be approximated as follows:

$$\mathrm{Re}\,\tilde{\Phi} \simeq C_{\mathrm{t}} N_{\mathrm{t}}(\varepsilon_{\mathrm{f}}) \int_0^\infty \frac{\tau_{\mathrm{r}}(\varepsilon)\,\mathrm{d}\varepsilon}{[1 + \omega_{\mathrm{f}}\tau_{\mathrm{r}}(\varepsilon)]^2} \simeq C_{\mathrm{t}} N_{\mathrm{t}}(\varepsilon_{\mathrm{f}}) \frac{kT}{\omega_{\mathrm{f}}}, \tag{B.3}$$

$$\begin{aligned}\mathrm{Im}\,\tilde{\Phi} &\simeq -\omega C_{\mathrm{t}} N_{\mathrm{t}}(\varepsilon_{\mathrm{f}} + kT\ln 2) \int_0^\infty \frac{\tau_{\mathrm{r}}^2(\varepsilon)\,\mathrm{d}\varepsilon}{[1 + \omega_{\mathrm{f}}\tau_{\mathrm{r}}(\varepsilon)]^3} \\ &\simeq -\omega C_{\mathrm{t}} N_{\mathrm{t}}(\varepsilon_{\mathrm{f}} + kT\ln 2) \frac{kT}{2\omega_{\mathrm{f}}^2}.\end{aligned} \tag{B.4}$$

Then, from the formulae (16) and (17) one gets the expressions (24) and (25).

Appendix C. Expression for MPC in the case of meaningful carrier diffusion and fast carrier neutralization at the collecting electrode

We shall give here the solution of equation (9), provided that the free carriers are very quickly neutralized on the collecting electrode. The corresponding boundary condition has the form of

$$\Delta n(d) = 0. \tag{C.1}$$

Determining the coefficients C_1 and C_2 in the general solution (30) from the conditions (33) and (C.1) one obtains

$$\Delta n(x) = \frac{\Delta i_{\text{in}}[\exp(-\lambda_1 x - \lambda_2 d) - \exp(-\lambda_2 x - \lambda_1 d)]}{e D_0[\lambda_1 \exp(-\lambda_1 d) - \lambda_2 \exp(-\lambda_2 d)]}. \tag{C.2}$$

Inserting this expression into equation (11) yields the following formula for the MPC:

$$\Delta I = \frac{\Delta I_0}{d[\lambda_1 \exp(-\lambda_1 d) - \lambda_2 \exp(-\lambda_2 d)]} \times \left\{ \frac{\mu_0 E_0}{D_0} \left\{ \frac{1}{\lambda_1}[1 - \exp(-\lambda_1 d)] \exp(-\lambda_2 d) - \frac{1}{\lambda_2}[1 - \exp(-\lambda_2 d)] \exp(-\lambda_1 d) \right\} - \exp(-\lambda_1 d) + \exp(-\lambda_2 d) \right\}. \tag{C.3}$$

Appendix D. Erratum to I

In I there is an error in equation (B.3). This equation should be

$$\frac{\mu_0 E_0(x)}{1 + \tilde{\Phi}(x)} \frac{\mathrm{d}\Delta E(x)}{\mathrm{d}x} + \left[\mathrm{i}\omega + \frac{1}{\tau_M(x)} \right] \Delta E(x) = \frac{e}{\kappa \kappa_0} \int_0^x \Delta g(x')\, \mathrm{d}x' + \mathrm{i}\omega \Delta E(0).$$

We apologize for the mistake.

References

[1] Oheda H 1981 *J. Appl. Phys.* **52** 6693
[2] Brüggemann R, Main C, Berkin J and Reynolds R 1990 *Phil. Mag.* B **62** 29
[3] Hattori K, Niwano Y, Okamoto H and Hamakawa Y 1991 *J. Non-Cryst. Solids* **137/138** 363
[4] Hattori K, Iida M, Hirao T and Okamoto H 2000 *J. Appl. Phys.* **87** 2901
[5] Longeaud C and Kleider J P 1992 *Phys. Rev.* B **45** 11672
[6] Longeaud C and Kleider J P 1993 *Phys. Rev.* B **48** 8715
[7] Reynolds S, Main C, Webb D P and Grabtchak S 2000 *J. Appl. Phys.* **88** 278
[8] Kounavis P 2001 *Phys. Rev.* B **64** 045204
[9] Kounavis P and Mytilineou E 1999 *J. Phys.: Condens. Matter* **11** 9105
[10] Brüggemann R and Kleider J P 2002 *Thin Solid Films* **403/404** 30
[11] Schumm G and Bauer G H 1989 *Phys. Rev.* B **39** 5311
[12] Brüggemann R, Schumm G, Main C, Berkin J and Bauer G H 1991 *J. Non-Cryst. Solids* **137/138** 359
[13] Amato G, Giorgis F, Fizzotti F and Manfredotti C 1993 *Solid State Commun.* **86** 277
[14] Cohen J D and Zhong F 1995 *J. Non-Cryst. Solids* **190** 123
[15] Naito H 1996 *J. Appl. Phys.* **80** 5089
[16] Grygiel P, Tomaszewicz W and Wiśniewski G 2000 *Visnyk Lviv Univ. Ser. Phys.* **33** 219
[17] Tomaszewicz W 1990 *Phil. Mag. Lett.* **61** 237
[18] Hattori K, Adachi Y, Anzai M, Okamoto H and Hamakawa Y 1994 *J. Appl. Phys.* **76** 2841
[19] Grygiel P and Tomaszewicz W 2000 *J. Phys.: Condens. Matter* **12** 5209